Motor Control with Active Impedance of the Driver

B. J. Lurie*, B. Dolgin*, and F. Y. Hadaegh†
Jet Propulsion Laboratory, California Institute of Technology,
4800 Oak Grove Dr., Pasadena, Ca 91109

Abstract. Making the driver output impedance active allows reducing the sensitivity of the motor angular velocity to variations of the load parameters. Compensating the voltage drop on the motor winding, and making the output impedance of the driver the negative of the impedance of the motor winding are the two potentially equivalent design methods considered in this paper. Performances of the systems using a current driver, a voltage driver, and a driver with active output impedance are compared in applications to antenna pointing and to rower wheel control.

1. Motor angular velocity

A permanent magnet dc motor is described by equations

$$\tau = kI, \tag{1}$$

$$E = (Z_d + Z_w)I + k\Omega; \tag{2}$$

here, Ω is the motor angular velocity, τ is the torque, k is the motor constant, i.e. the ratio of the torque to the applied current I, and E is the emf at the output of the driver. Z_d is the driver's output impedance, Z_w is the impedance of the motor winding, and $k\Omega$ is the back emf.

The ratio $Z_L = \Omega/\tau$ is the motor load mobility. The load mobility includes the load dynamics and may include friction. It is to a large degree uncertain, and its variations affect the motor velocity.

From (1),(2), the input impedance of the motor is $Z_w + Z_L/k^2$.

From (1),(2)

$$\Omega = \frac{\frac{E}{k}}{1 + \frac{Z_d + Z_w}{Z_L k^2}} \tag{3}$$

and the sensitivity of the velocity Ω to the load mobility Z_L is

$$S_\Omega = \frac{\frac{d\Omega}{\Omega}}{\frac{dZ_L}{Z_L}} = \frac{1}{1 + \frac{Z_L k^2}{Z_d + Z_w}} \quad . \tag{4}$$

It is seen that the sensitivity depends on Z_d and vanishes when $Z_d = -Z_w$. Therefore, proper shaping the frequency response of Z_d is important.

---

* Member of Technical Staff, †Senior Research Scientist

$|Z_w|$ in high efficiency motors is typically much smaller than the typical electrical load impedance k^2Z_L. When using a voltage driver, Z_d is 0. In this case the second component in the denominator of (3) is smaller than 1 (typically, 0.1 to 0.3), and the effects of the load uncertainty and the friction reflected in the variations of Z_L are reduced, compared to the case of using a current driver when $|Z_d|$ is big, the motor current is $I = E/Z_d$, the velocity $\Omega = IkZ_L$ is directly proportional to Z_L, and the sensitivity (4) is 1.

If $Z_d + Z_w = 0$, the velocity $\Omega = E/k$ and the sensitivity (4) turns to 0; the independence of the angular velocity from uncertain dynamic loads Z_L and from the bearing friction is highly desirable. It has been demonstrated (e.g. in [1]) that this property can be achieved over a limited frequency range by some schemes compensating the effect of Z_w, and the impedance compensation has been employed in some industrial motor control systems. However, it is not used universally because of the lack of a convenient methodology for the design of this complex multiloop system and calculating the available benefits.

2. Outer loop

The plant angle θ_T is commonly controlled closed-loop via an outer loop with an angle (or rate) sensor. It is typically close to the motor shaft angle $\theta = \Omega/s$ over the operational frequency range but, when the plant is flexible, can differ at higher frequencies due to structural modes.

The feedback in the outer loop is limited by several factors [2,3,4]: plant parameter uncertainty including structural modes, sample frequency, quantizing of the sensors (the sensors used for the angle control are most often digital like the optical encoder). In many cases, only the one numerically strictest of these limitation counts. However, in some other cases, the cumulative effect of these factors is much more severe than each of these limitation taken separately.

For example, the effect of a structural resonance can be alleviated by properly shaping the Bode diagram to provide phase-stabilization at the resonance frequency. And, if the feedback is collocated, the structural resonances are automatically phase-stabilized. However, when the sample frequency is relatively low (less than 5 time higher than the structural resonance frequency), it creates large additional phase uncertainty at the resonance frequency which prevents phase stabilization. In this case, this mode has to be gain-stabilized which reduces the feedback bandwidth (up to by a couple of octaves) and substantially reduces the feedback and the disturbance rejection.

Also, quantization of the sensor readings together with low sampling rate requires lowering the feedback bandwidth more than each of this factors taken separately.

Making the driver impedance active can substantially improve the disturbance rejection in these cases. When the contour impedance in the driver loop is made zero, the structural resonances do not affect the outer loop, and the feedback bandwidth in the outer loop f_b becomes only limited by the sampling frequency, $f_b < 0.1 f_s$.

The tachometer rate sensor, although not as precise, is analog and is collocated thus allowing for wide bandwidth of the rate feedback and for large disturbance rejection. Using the rate feedback with a tachometer winding reduces the effects of friction and cogging, reduces therefore the parameter variations for the plant of the outer loop, and allows increasing the feedback in the digital sensor loop. Combining the analog tachometer rate feedback and digital encoder angle feedback benefits the provision of high accuracy control.

However, the tachometer winding occupies some space that otherwise can be utilized to increase the diameter of the wires in the main motor winding. For this and other reasons, permanent magnet motors rarely have separate tachometer windings.

The performance of a system using a driver with prescribed active output impedance are comparable with that of a system having a tachometer.

3. Compensation of the voltage drop on the motor winding impedance

Compensating the effect of the winding impedance rendered by the actuator feedback is shown in Fig. 1. The feedback uses a small impedance $0.5Z_w/D$ as a current sensor. The fed back signal is applied to the input of the summing amplifier in phase with the incident signal. The amplifier gain coefficient from the feedback input is 2. Due to this feedback, the emf at the output of the driver amplifier increases by IZ_w. This increment equals the voltage drop on the winding impedance Z_w. Thus, the compensating feedback makes the motor current to be the same as it would be if $Z_w = 0$. The forward path can be therefore seen as cascade connection of C and the block D/k, as shown in Fig. 1(b). Thus, when the sensing impedance is exactly $0.5Z_w/D$, the velocity $\Omega = CD/k$ is independent of the load. When the compensation is not exact but close to it, the sensitivity (4) is not 0 but small, much less than 1. Closing the outer loop further improves the control accuracy.

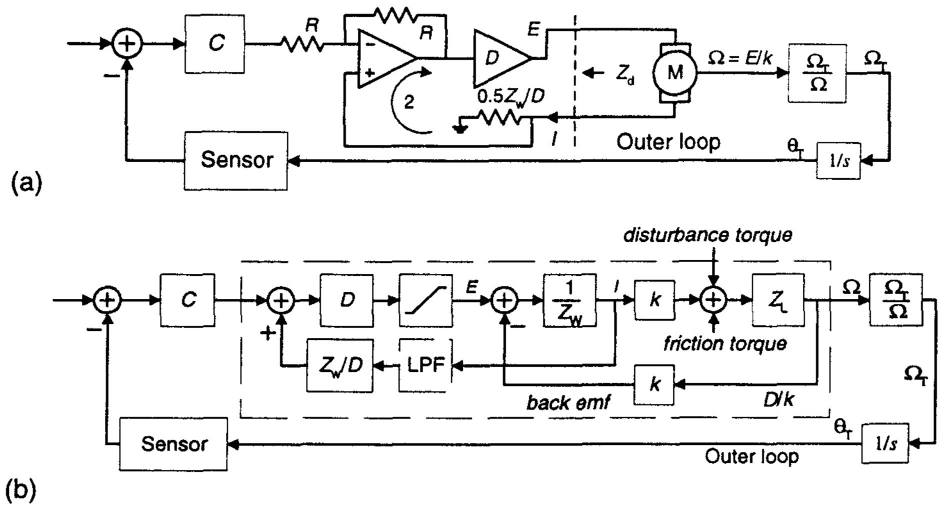

Fig. 1 Feedback loop compensating voltage drop on the motor winding impedance, (a) simplified schematic diagram, (b) block diagram

The compensating feedback path changes the output impedance of the driving circuit. We can consider the circuit to the left of the vertical dashed line in Fig. 1(a) as a new driver amplifier. Since with this new driver amplifier the effect of Z_w is eliminated, then, in accordance to (3),(4) the output impedance of the new driver must be $Z_d = -Z_w$.

The system in the dashed box in Fig. 1(b) has two crossed loops. The loop gain in the first loop is 1 and the return difference is 0; with this loop closed, the loop gain in the second, the back emf loop, is infinite. Due to this, the transfer functions from the disturbance torque and the friction torque to Ω and Ω_T are 0.

The feedback path transfer coefficient cannot be exactly Z_w/D at all frequencies. The system stability requires the feedback path to include a low-pass filter LPF. This reducing the system precision.

Thus, we can identify the application areas where these methods can be most useful: motors without tachometer windings, flexible plants, digital angle sensors, and outer loops with noncollocated control at higher frequencies.

4. Active output impedance of the driver

The effect of Z_w can be compensated by Z_d approximating $-Z_w$ so that (3) reduces to $\Omega \approx E/k$. This can be done by application of large compound feedback about the driver as shown in Fig. 3. The voltage feedback coefficient is β_V and the current feedback coefficient $\beta_I = \beta_V Z_a$, where Za is the current sensor impedance.

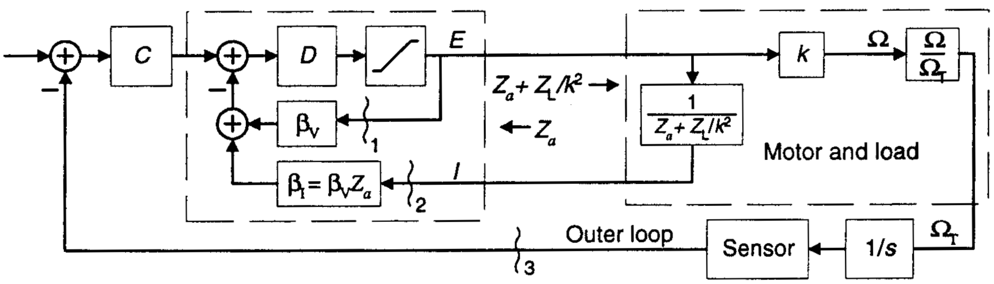

Fig. 3 Feedback control with large gain driver amplifier and prescribed output impedance of the actuator

Over the frequency range where the driver amplifier gain coefficient D is large, the output impedance can be calculated using Blackman's formula [2,4] as $Z \approx \beta_I/\beta_V$ and it depends only on the feedback path coefficients in the current and voltage loops which can be implemented with high precision.

A particular case is the case of a voltage driver.

Using a voltage driver is shown in Fig. 5. The voltage driver can be thought of as an infinite gain amplifier (i.e. $D = \infty$) with unity voltage feedback path. Then, $\beta_V = 1$, and to get the required output impedance Z_a, the current feedback path coefficient should be Z_a. By using the link with transfer function $Z_a = -Z_w$, the driver output impedance $-Z_w$ can be obtained, and the gain coefficient from E to Ω becomes $1/k$.

As should be expected, this approach results in the diagram in Fig. 1(b) which was obtained with the actuator feedback compensating the voltage drop.

Notice that Z_a must equal $-Z_w$ only over the frequency range of importance. Outside of this range the impedance frequency response must be shaped such that the system is stable and robust.

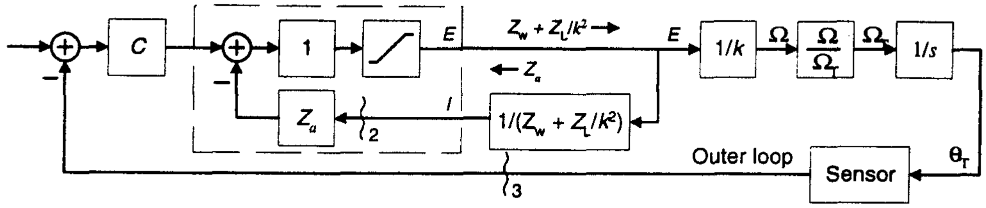

Fig. 5 Feedback control with voltage driver and prescribed output impedance of the actuator

5. A servo with a voltage driver and a current compensating feedback loop

Consider an antenna pitch control system where the digital encoder angle sensor mounted on the motor shaft close to the motor. The control is collocated. The sampling frequency is 400 Hz, so the Nyquist frequency is 200 Hz.

The motor with the moment of inertia of the rotor $J_R = 0.001$ kgm^2 rotates an antenna with the moment of inertia $J_A = 0.01$ kgm^2 via a shaft. The frequency of the free-free torsional resonance of the antenna on the shaft is 200 Hz, i.e. 1260 rad/sec. The damping of the structural resonance is 1%, i.e. the resonance peak is 40 dB high.

In the absence of friction, the mobility of the motor load is

$$Z_L = \frac{1}{0.01s} \times \frac{s^2 + 20s + 1150^2}{s^2 + 25.2s + 1260^2} \times \frac{1260^2}{1150^2} .$$

Current driver. When the driver is a current one, the output mobility of the motor becomes infinity and the load mobility becomes a multiplier in the loop transfer function. The pole frequency of the structural resonance is close to the Nyquist frequency, therefore the loop phase shift at this frequency becomes completely unpredictable and the loop should be gain-stabilized. In this case when the loop response is implemented with the major slope of −10 dB/oct, with Bode step [2,3,4], with 10 dB and 30° stability margins, and with the asymptotic slope −18 dB/oct, the crossover frequency is 22 Hz as seen in Fig. 9. The loop gain at 5 Hz is 10 dB. The feedback attenuating the 10 Hz frequency component of the disturbances caused by the friction is about 9 dB.

Voltage driver. Assume the motor constant $k = 0.8$, the winding resistance is 4 Ω, and the winding inductance is 1 mH. The output mobility of the motor becomes $k^2 Z_w = 2.5$ at dc and $2.5\angle 20°$ at the frequency of the structural resonance.

The load mobility at the frequency of the structural resonance is $Q/(J\omega) = 100/(0.01\omega) = 8.0$. The mobility of the parallel connection of the load and the driver decreases to 1.9, i.e. the peak decreases by $20\log(8/1.9) = 13$ dB. Hence, the loop Bode diagram can be shifted toward high frequencies by $13/18 = 0.7$ octaves. The crossover frequency becomes 16 Hz, the loop gain increases by 7 dB (in accordance with the −10 dB/oct main slope), and the feedback becomes 18 dB. In addition to this 8 dB improvement of the friction disturbance rejection, the disturbance is also reduced by the back-emf feedback loop, approximately by 10 dB. Therefore, using a voltage driver allows improving the disturbance rejection by 18 dB compared to using a current driver.

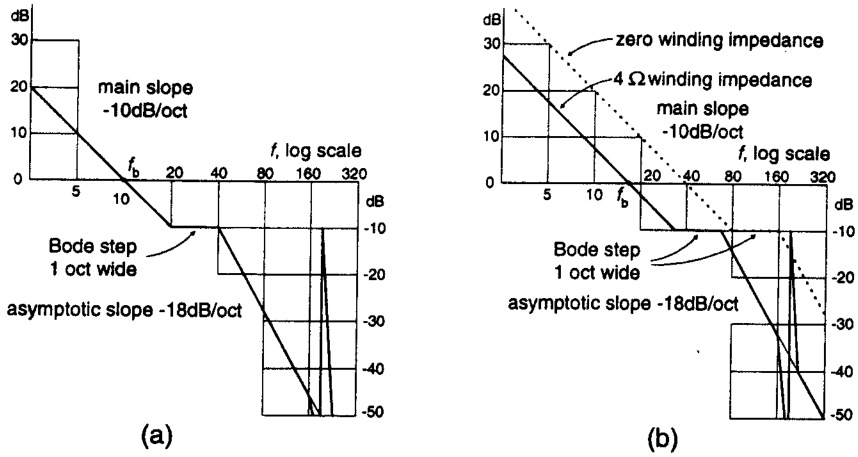

Fig. 9 Outer loop piece-linear Bode diagrams (a) with current driver, (b) with voltage driver

Voltage driver with zero motor winding impedance. Would the winding impedance be zero at all frequencies, the gain in the back-emf feedback loop becomes infinite, and the ratio of the rate to the signal at the output of the compensator becomes $1/k = 1.22$. The disturbance rejection becomes infinite.

The plant structural resonance completely disappears, and the outer loop feedback bandwidth becomes limited by only the sampling frequency, i.e. $f_b \leq 0.1 \times 400 = 40\,\text{Hz}$. The outer feedback at 5 Hz achieves 30 dB, i.e. becomes 12 dB bigger than that for the voltage driver.

Voltage driver with in-phase current feedback. A block diagram for the system with no outer loop is shown in Fig. 10. A voltage driver is enlooped with a current in-phase feedback. According to Blackman's formula, the contour impedance $Z_w(1 - 0.03*100/Z_w) = 1 + 0.001s$. The pole of the actuator-and-plant transfer function is, approximately, at the frequency where the load mobility is $-j1\,\Omega$, i.e. at 100 rad/sec.

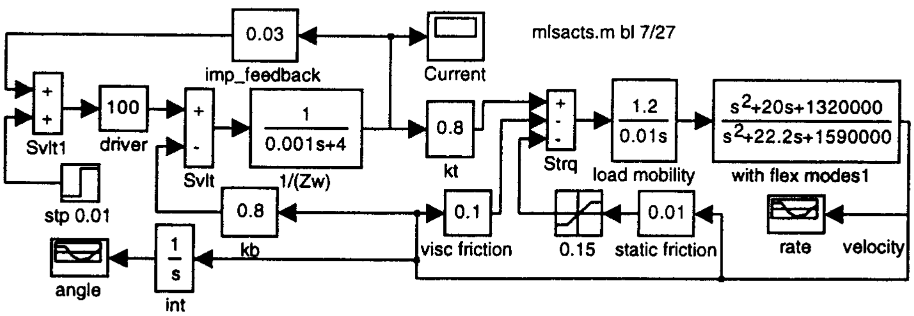

Fig. 10 SIMULINK diagram of the system without the outer loop

The actuator and plant transfer function $AP \approx 15{,}000{,}000/[(s + 70)(s + 1800)s]$. For the frequency components below 50 rad/sec (i.e. for the times over 0.05 sec) the AP performs as an integrator. When a unit step is applied to the voltage summer at 0.1 sec, the rate time-response is close to $1/k$ times the step, and the output angle time-response is a ramp of $1.1t$ as seen in Fig. 11.

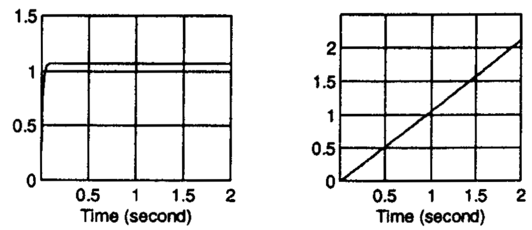

Fig. 11 Rate and angle responses of AP to voltage step

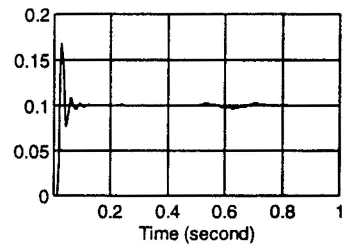

Fig. 12 Closed loop response

The transfer function for the outer loop compensator can be presented as $T/(AP) = Ts^3 \times 1/(APs^3) \approx Ts^3 \times (s + 70)(s + 1800)/(1.5E7ss) = (10^{-7}Ts^3) \times 0.667(s + 70)(s + 1800)/ss$, where and the loop transfer function with $f_b = 30$ Hz and a Bode-step [2,3,4]

$$T(s) = \frac{-7.37e7s^4 + 6.94e10s^3 + 1.05e14s^2 + 4.77e16s + 3.04e18}{s^5 + 3336s^4 + 3.94e6s^3 + 2.93e9s^2 + 1.33e12s + 1.97e14} \frac{1}{s^2}.$$

In the control system with the outer loop, the disturbance of one wave of sinusoidal 5 Hz oscillation starts at the time of 0.5 sec. The transient response is shown in Fig. 12 (the overshoot can be reduced by an appropriate prefilter [4]).

7. Application to rover motion and drilling

The motor torque components caused by the gravity depends on the path inclination (e.g. when the rover rolls over a boulder) can be viewed as torque disturbances.

When driven by a current driver, the motor is a torque source, and the uncertain plant mobility enters the loop transfer function as a multiplier. In this case of the loop feedback bandwidth is constraint and may be insufficient for the required control accuracy of the wheel rate. On the other hand, when the driver is voltage and the motor winding impedance is small, the motor rate is commanded by the input of the driver, the plant impedance and friction do not affect the loop transfer function, and the required rate accuracy is much better. When the motor winding impedance is substantial, making the driver output impedance negative should substantially improve the accuracy of the rover motions over a complex terrain, and the speed of the rover can be increased.

Using the driver with active impedance must also improve the performance of the servos controlling the drilling mechanism placed on the rover for the purpose of sample taking.

Acknowledgment. The research was carried out by the Jet Propulsion Laboratory, California Institute of Technology, under a contract with the National Aeronautic and Space Administration.

References

1. A. M. Wooster, Control Circuit Keeps DC Motor Running At Constant Speed, Electronic Design, March 23, 1998.
2. B. J. Lurie, *Feedback Maximization*, Artech House, Dedham, MA: 1986.
3. B. J. Lurie, A. Ghavimi, F. Y. Hadaegh, E. Mettler, System trades with Bode step loop response, AIAA Guidance and Control Conference, Boston, Aug. 1998.
4. B. J. Lurie and P. J. Enright, *Classical Feedback Control*. Marcel Dekker, N.-Y., 2000.